Analysis of LVRT scenarios within a complete system model of a DFIG wind turbine

Christoph Mülder[1]
Kay Hameyer[1]

[1]Institute of Electrical Machines (IEM)
Schinkelstraße 4, 52062 Aachen, Germany

Contents

1 Abstract

The purpose of this paper is to study grid fault scenarios by the multi-physical simulation environment *DYMOLA* to analyze both electrical and mechanical loads during particular events.

Therefore, an overall system model is described by several subcomponents consisting of the wind turbine, mechanical drive train, electrical machine and its control. Since doubly fed induction generators are directly coupled to the grid, fault scenarios must be considered in the design of both electrical and mechanical turbine equipment. Particularly the power semiconductors of the converter enabling a speed-variable operation of the turbine must be protected in the failure case. Such protection equipment is often realized by crowbar systems which have been studied further in this work. Exemplary the simulation setup is studied by a low-voltage ride through scenario where different crowbar resistances are analyzed. It can be concluded that the impact of the protection system setup on electrical and mechanical loads differ and must be taken into account already at the design stage of DFIG wind turbines. It is shown that *DYMOLA* represents a promising simulation environment to identify system effects, e.g. for the mentioned failure cases.

2 Introduction

Wind turbines with doubly fed induction generators (DFIG) are a well-known concept for the electromechanical energy conversion of wind. The structure of the system consisting of many partial components lead to a complicated problem in terms of predictive modelling at the design stage.

Fault-ride-through (FRT) scenarios of the grid, e.g. the low-voltage-ride-trough (LVRT), need to be overcome successfully by the wind turbine according to grid codes. Besides the capability of grid support in a faultive case, the turbine should pass through without any component damage. The occurrence of high fault currents in a LVRT-scenario can lead to a destruction of the rotor side converter (RSC). Moreover, the resulting torques and forces stress the drive train, e.g. the gear, because of the direct coupling with the grid through the stator of the generator. An accurate modelling of the complete system behavior is therefore indispensable and will be discussed in the course of this work. Load-reducing methods are evaluated in addition.

3 Methods

3.1 System model in *DYMOLA*

In Figure 1 the overview of the overall system model of a wind turbine with a DFIG in is illustrated. The physically sounded simulation environment *DYMOLA* with its programming language *MODELICA* offers the possibility to model the physical behavior of each sub system in variable depth of detail [EBE15]. Besides the modularity, multi-physical problems with time constants in different scale can be solved very convenient.

The system consists of several subcomponents coupled by mathematical and physical based interfaces represented by differential equations describing the behavior in the time domain. In the following subchapter the model equations are introduced.

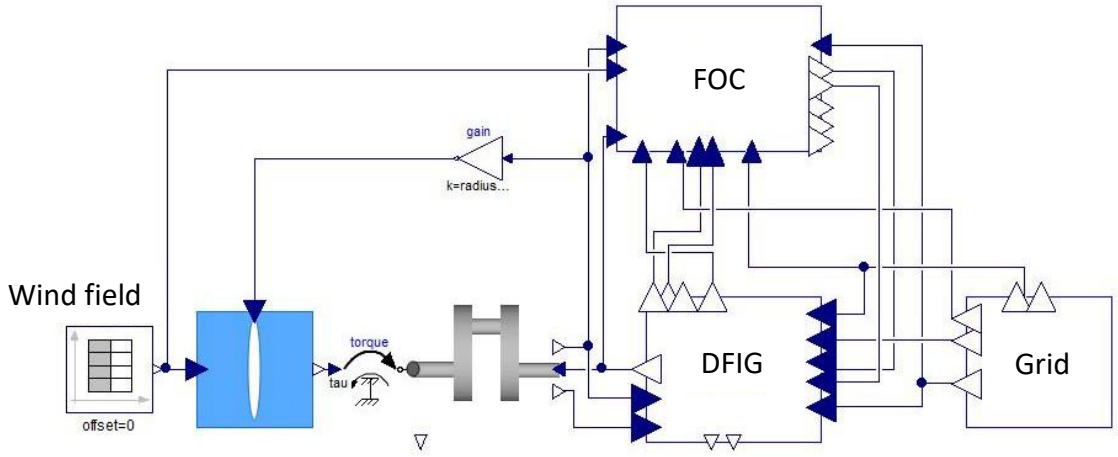

Figure 1: Overview of the overall system model in DYMOLA with subcomponents.

3.2 Model components

The first subsystem in Figure 1 represents a wind field generator and the wind rotor of the turbine (illustrated by a blade). The torque of the wind acting on the turbine [KLE93]

$$M_{\mathrm{T}} = \frac{c_{\mathrm{p}}}{\lambda}\frac{\pi}{2}\rho_{\mathrm{air}}R_{\mathrm{T}}^{3}v_{\mathrm{wind}}^{2} \qquad \textbf{Eq. 1}$$

can be deduced by the well-known laws of aeromechanical power conversion with the wind speed $\boldsymbol{v_{\mathrm{wind}}}$,the air density $\boldsymbol{\rho_{\mathrm{air}}}$ (assumed as constant), the radius of the turbine (representing the length of one blade) $\boldsymbol{R_{\mathrm{T}}}$ and the power coefficient

$$c_{\mathrm{P}}(\lambda,\beta) = c_1\left(\frac{c_2}{\lambda} - c_3\beta - c_4\right)e^{-\frac{c_5}{\lambda}} \qquad \textbf{Eq. 2}$$

depending on the tip speed ratio λ and the pitch angle β. c_1-c_5 are model parameter which can be obtained for arbitrary blade profiles. The Betz' limit represents the theoretical upper limit of the aeromechanical energy conversion with $c_{\mathrm{P,max}} = \frac{16}{27} \approx 0.592$.

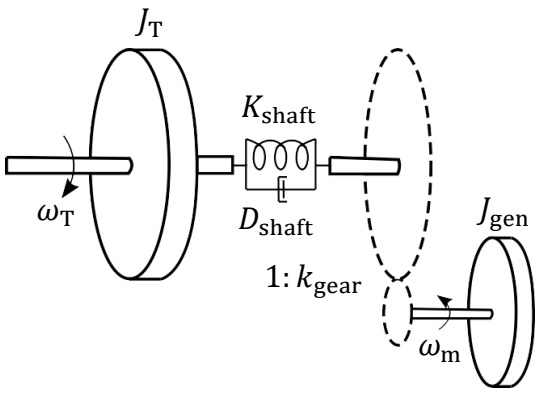

Figure 2: Illustration of the drive train as a mechanical double oscillator.

The torque M_T of the turbine is then coupled to the mechanical drive train illustrated in Figure 2. The drive train can be modeled for the first rotational degree of freedom by a double oscillator coupled by spring damper elements [RIC17].

The gearbox is assumed being a lossless transmission element between the low- and the high-speed shaft with the rotational speeds ω_T and ω_m. The moments of inertia of both sides are represented by J_T and J_gen.

The electromagnetic behavior of the DFIG is modeled by the standard circuit equivalent of an induction machine. The voltage equations in the stator voltage oriented dq-reference frame is [ABA11]:

$$\frac{\mathrm{d}}{\mathrm{d}t}\begin{bmatrix} i_\mathrm{ds} \\ i_\mathrm{qs} \\ i_\mathrm{dr} \\ i_\mathrm{qr} \end{bmatrix} = \left(\frac{1}{\sigma L_\mathrm{r} L_\mathrm{s}}\right)\tilde{A}\begin{bmatrix} i_\mathrm{ds} \\ i_\mathrm{qs} \\ i_\mathrm{dr} \\ i_\mathrm{qr} \end{bmatrix} + \left(\frac{1}{\sigma L_\mathrm{r} L_\mathrm{s}}\right)\tilde{B}\begin{bmatrix} v_\mathrm{ds} \\ v_\mathrm{qs} \\ v_\mathrm{dr} \\ v_\mathrm{qr} \end{bmatrix} \qquad \textbf{Eq. 3}$$

with

$$\tilde{A} = \begin{bmatrix} -R_\mathrm{s}L_\mathrm{r} & \omega_\mathrm{m}L_\mathrm{m}^2 + \omega_\mathrm{s}\sigma L_\mathrm{s}L_\mathrm{r} & R_\mathrm{r}L_\mathrm{m} & \omega_\mathrm{m}L_\mathrm{m}L_\mathrm{r} \\ -\omega_\mathrm{m}L_\mathrm{m}^2 - \omega_\mathrm{s}\sigma L_\mathrm{s}L_\mathrm{r} & -R_\mathrm{s}L_\mathrm{r} & -\omega_\mathrm{m}L_\mathrm{m}L_\mathrm{r} & R_\mathrm{r}L_\mathrm{m} \\ R_\mathrm{s}L_\mathrm{m} & -\omega_\mathrm{m}L_\mathrm{m}L_\mathrm{s} & -R_\mathrm{r}L_\mathrm{s} & -\omega_\mathrm{m}L_\mathrm{s}L_\mathrm{r} + \omega_\mathrm{s}\sigma L_\mathrm{s}L_\mathrm{r} \\ \omega_\mathrm{m}L_\mathrm{m}L_\mathrm{s} & R_\mathrm{s}L_\mathrm{m} & \omega_\mathrm{m}L_\mathrm{s}L_\mathrm{r} - \omega_\mathrm{s}\sigma L_\mathrm{s}L_\mathrm{r} & -R_\mathrm{r}L_\mathrm{s} \end{bmatrix}$$

and

$$\tilde{B} = \begin{bmatrix} L_\mathrm{r} & 0 & -L_\mathrm{m} & 0 \\ 0 & L_\mathrm{r} & 0 & -L_\mathrm{m} \\ -L_\mathrm{m} & 0 & L_\mathrm{s} & 0 \\ 0 & -L_\mathrm{m} & 0 & L_\mathrm{s} \end{bmatrix},$$

where s and r are the indices for the stator and rotor components. L_m, L_r and L_s are the main-, rotor and stator inductances, σ the total leakage coefficient, R_s and R_r the stator and rotor resistance related to the stator side. The angular frequency of the grid voltage $\omega_\mathrm{s} = 2\pi\ 50\ \mathrm{Hz}$ and assumed to be constant.

The torque of the generator in the introduced dq-reference frame is calculated by

$$\mathrm{M_{gen}} = -\frac{3}{2} p \frac{L_\mathrm{m}}{L_\mathrm{s}} \frac{\widehat{V}_\mathrm{g}}{\omega_\mathrm{s}} i_\mathrm{qr}\,, \qquad \textbf{Eq. 4}$$

where $\widehat{V}_\mathrm{g}$ is the amplitude of the grid phase voltage and p is the number of pole pairs of the generator.

In Figure 3 the control scheme of the generator for the voltage-oriented control is illustrated. The reference values on the left-hand side of the control scheme are the setpoint of the torque M^*_gen and reactive power Q^*_s fed by the stator into the grid.

The control scheme can be divided into three separated blocks marked by the numbers in Figure 3. In the first block, the control variables are calculated by measured quantities of the generator and the grid. These variables are compared in the second block to the setpoints deduced by the turbine system control and controlled by a proportional-integral (PI) controller and the dq-components of the rotor current are calculated. In the third block, a PI controller finally derives the dq- components of the rotor voltage passed to the rotor side converter (RSC).

The grid block in Figure 1 is represented by a three-phase voltage source with constant frequency. This block is directly coupled to the DFIG block since the stator of the machine is directly connected to the grid voltage. Therefore, the control of the machine has to be designed with regard to sudden gird faults the turbine needs to ride through without any serious damages. Additionally, grid operators require steadily increasing capabilities of the grid side converter (GSC) regarding reactive power supply in case of a failure, in such way that the power rating of the converters has to be adapted [HOW16].

In the next subchapter simulation results based on low-voltage ride-through (LVRT)-scenarios will be presented.

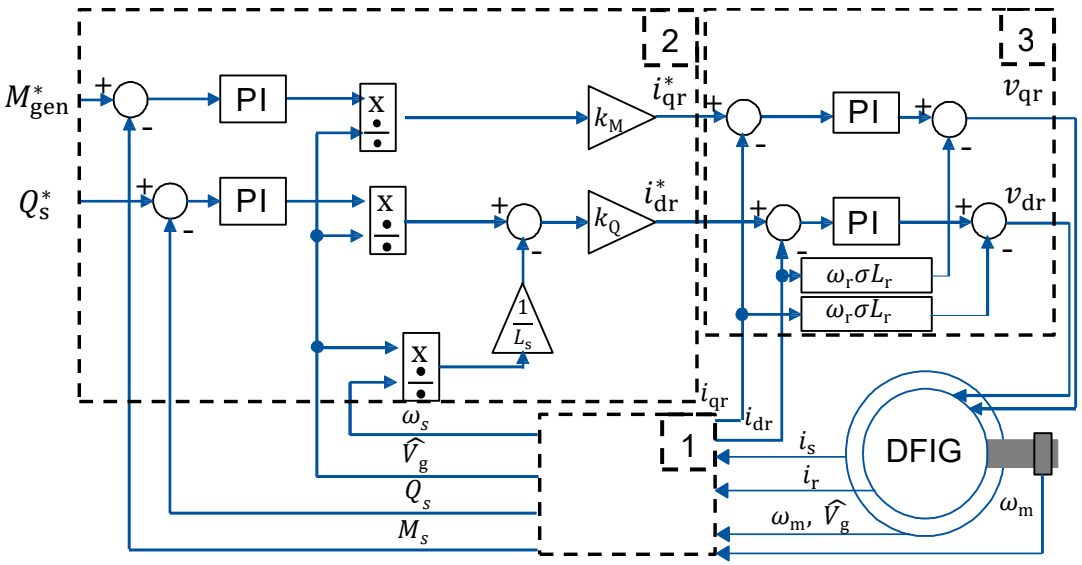

Figure 3: Control scheme of field-oriented generator control.

4 Simulation of fault scenario

In this subchapter the simulation scenario obtained from the overall system model of the DFIG wind turbine are presented based on a 80 % three-phase grid voltage dip as illustrated in Figure 4. The dashed curve represents the boundary required by grid codes, on which basis wind turbine operators are forces to stay connected to the grid [BDE08]. This voltage drop is kept for 150 ms. The grid voltage recovers after 250 ms and stays constant then at its rated value.

Grid fault scenarios as the studied low-voltage ride-through result in high currents, in both the stator and rotor winding. Particularly in the rotor circuit, this can lead to a destruction of the power semiconductors of the converter resulting probably in a downtime of the turbine. To prevent the components, a commonly used protection equipment is a crowbar system as illustrated in Figure 5. This system ensures the stator of the DFIG to stay connected to the grid at the point of common coupling (PCC) during failure situation. The steps during the exemplary grid fault illustrated in Figure 4 are summarized [SAL10]:

1. Disconnection of the rotor windings from the RSC via circuit breaker (cf. Figure 5).
2. Insertion of the three-phase resistance in series to the rotor windings (CB).
3. Disconnection of CB from the rotor windings after fault recovery.
4. Reconnection of the RSC to the rotor windings.

Additionally, the grid side converter (GSC) on the one hand has to provide reactive power to the grid in terms of voltage stability. On the other hand, before proceeding with step 4 (reconnection), it has to control the DC-link voltage to ensure a stable operation of the DFIG. Particularly the torque of the machine has to be controlled to minimize the mechanical load in the drive-train during crowbar activation.

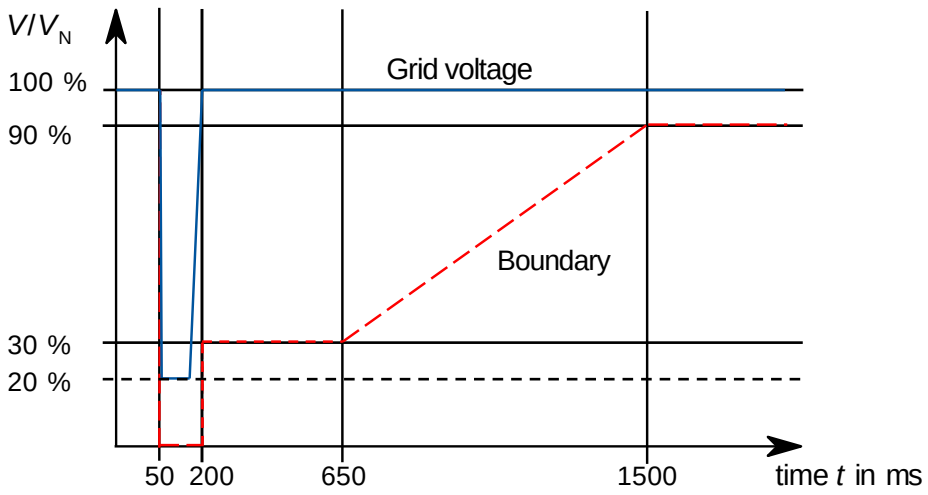

Figure 4: Grid voltage amplitude and boundary line according to grid code over time.

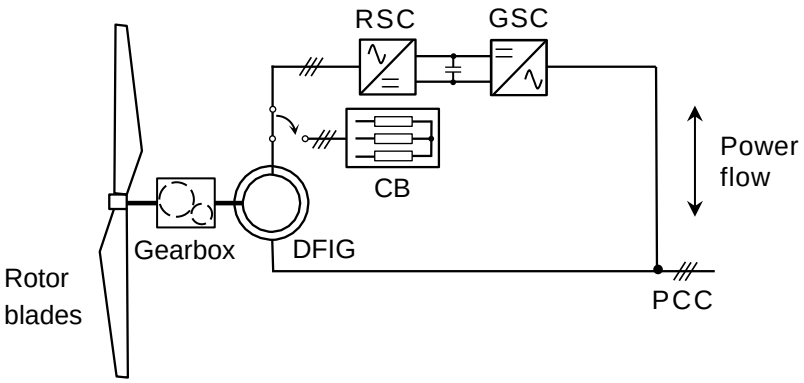

Figure 5: System overview of a turbine with DFIG, crowbar and circuit breaker.

5 Results and conclusions

In Figure 6 are the resulting rotor current waveforms of the three phases for different crowbar resistances plotted. It can be concluded that the maximum current amplitude in the rotor windings can be effectively reduced by about 40 %.

Moreover, high transient currents occur during the reconnection of the RSC. This results from the dynamic balancing process by the residual magnetizing field and the recovered grid voltage. For stable operation and reducing dynamic loads, this must be taken into account.

The torque and sped waveform of the HSS of the generator during the fault scenario is illustrated in Figure 7. It can be noted that both, the torque and speed do not change depending on the crowbar resistance. Immediately after the voltage drop, the torque decreases and oscillates around zero.

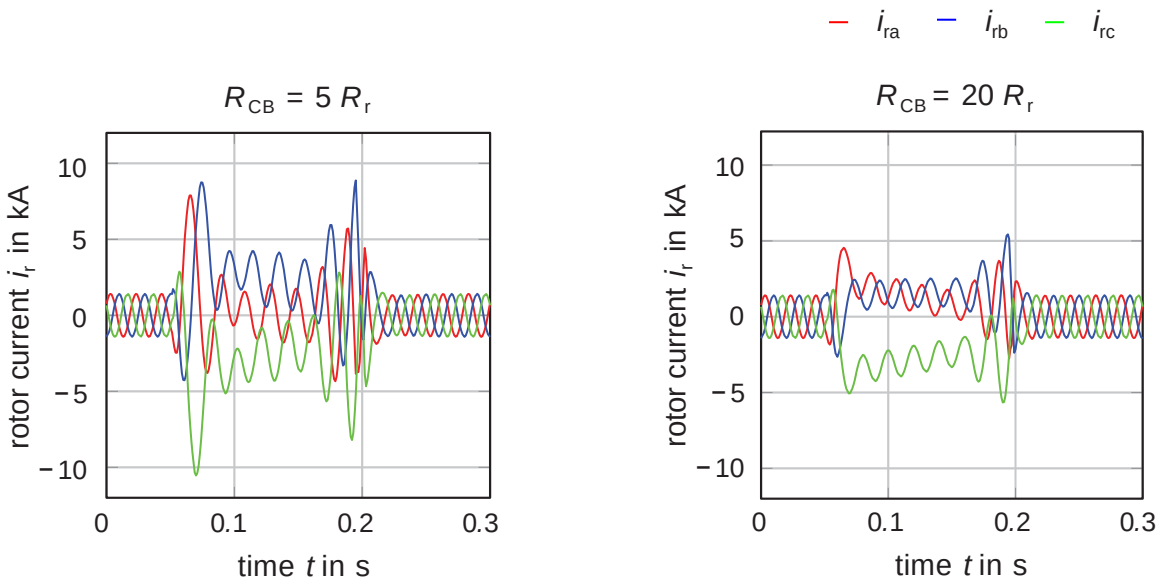

Figure 6: Rotor current waveforms in a LVRT scenario for different crowbar resistances.

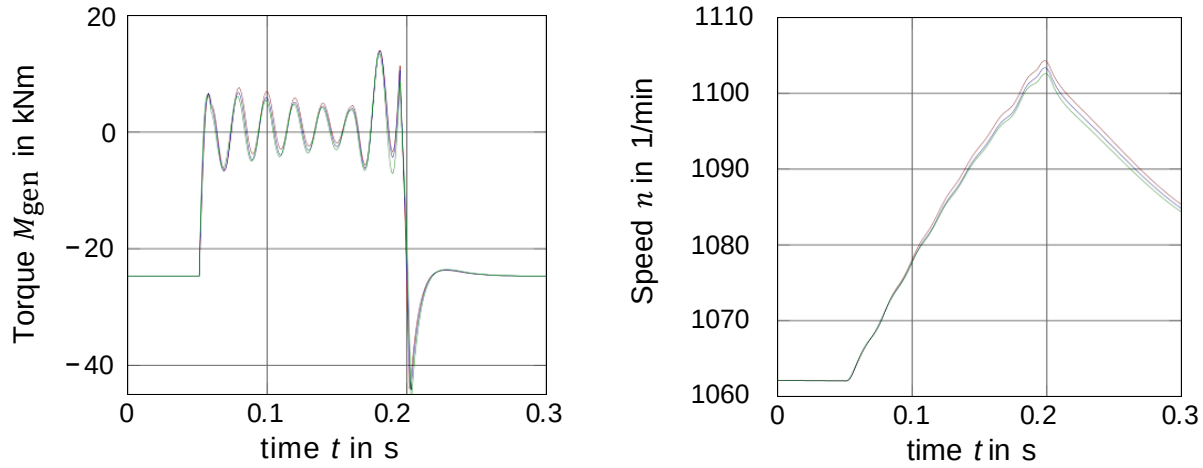

Figure 7: Generator torque and speed waveform during a LVRT scenario for different crowbar resistances.

Since the torque of the turbine stays approximately constant during the observed period of time of 300 ms, the turbine accelerates by approximately 50 rpm. After the voltage recovery, a transient torque peak can be noted. Since the torque corresponds to the airgap electromagnetic torque, one has to consider the mechanic transfer path of the shaft and the gearbox which was shown by a comparable measurement setup studying the use of crowbar during a converter failure [DUD18].

In future works, the identified effects will be considered to study local mechanical loads for the further understanding of damages in wind turbines equipped with DFIG. Mechanical and electrical loads can be analyzed by the multi-physical simulation environment *DYMOLA* offering promising interfaces to couple mechanical and electrical subcomponents.

6 Bibliography

[EBE15] Eberhart, P.; Shan Chung, T.; Haumer, A.; Kral, C.:
Open Source Library for the Simulation of Wind Power Plants.
In: Proceedings of the 11th International Modelica Conference, Versailles, France, 2015.

[RIC17] Rick, S.; Oberneder, M.; Hameyer, K.:
Torsional vibrations in multi-megawatt wind turbine induction generators.
In: Conference for Wind Power Drives 2017: Conference Transcript, Vol. 3, 2017.

[KLE93] Kleemann, M.; Meliß, M.:

Regenerative Energiequellen.

2nd Edition. Springer Berlin Heidelberg,1993

[ABA11] Abad, G.; López, J.; Rodríguez, M..; Marroyo, L..; Iwanski, G.:

Doubly fed induction machine: Modeling and control for wind energy generation applications.

Bd. 84. Hoboken: Wiley IEEE Press, 2011.

[HOW16] Howlader, A.; Senjyu; T.:

A comprehensive review of low voltage ride through capability strategies for the wind energy conversion systems.

In: Renewable and Sustainable Energy Reviews, vol. 56, pp. 643–658, 2016.

[BDE08] Bundesverband der Energie- und Wasserwirtschaft e.V.:

Technische Richtlinie Erzeugungsanlagen am Mittelspannungsnetz: Richtlinie für Anschluss und Parallelbetrieb von Erzeugungsanlagen am Mittelspannungsnetz.

Berlin, 2008.

[SAL10] Salles, M..; Hameyer, K.; Cardoso, J..; Grilo, A.; Rahmann, C.:

Crowbar System in Doubly Fed Induction Wind Generators.

In: Energies, vol. 3, no. 4, pp. 738–753, 2010.

[DUD18] Duda, T.; Jacobs, G and Bosse, D.:

Investigation of dynamic drivetrain behaviour of a wind turbine during a power converter fault.

In: Journal of Physics: Conference Series, Vol. 1037 No. 5, p. 52031, 2018.